Title
Coherent curvature radiation from an electron beam rotating in a plasma

Journal
Journal of Applied Physics, 50(10)

ISSN
00218979

Authors
Tzach, D.
Benford, Gregory
Roberson, C. W
et al.

Publication Date
1979

DOI
10.1063/1.325759

Peer reviewed

Coherent curvature radiation from an electron beam rotating in a plasma

D. Tzach, Gregory Benford, C. W. Roberson, and N. Rostoker
Physics Department, University of California, Irvine, California 92717

(Received 25 September 1978; accepted for publication 12 March 1979)

Microwave-radiation bursts at $\lambda \sim 1$ cm are observed when a rotating relativistic electron beam interacts with a plasma. The power level exceeds 1 MW, and the radiation pulse lasts as long as the electron beam pulse for beams up to 1 μsec long. The results are consistent with a model of coherent curvature radiation from electrons bunched due to a two-stream instability. Other mechanisms are ruled out by observations of harmonic splittings and the power spectrum.

PACS numbers: 52.40.Mj, 52.60. + h, 52.35.Py, 52.35.Hr

I. INTRODUCTION

It has been known since the first decades of this century that charged particles gyrating in a magnetic field radiate electromagnetic waves. [1–4] This synchrotron radiation explains many of the intense radio sources of astronomy. Until recently it was not realized that this process can be made collective, in the sense that correlations between the radiating particles enhance the power. This may occur naturally in pulsars, where the particles move along the curved field lines of the magnetosphere. This "coherent curvature radiation" is in fact a generalization of synchrotron radiation to the case where the radius of curvature of the orbit, ρ, is not from the Larmor orbit, but instead the instantaneous curvature of the local field lines. In both cases the physics is the same—enhancement of the single-particle radiation by bunching of the particles in the azimuth of the turning orbit. This spatial bunching of electrons most probably arises from a streaming instability between the relativistic electrons and a background plasma. In pulsars, the nature of the beam and plasma are conjectural since they cannot be observed. In the laboratory, however, we can make beams and plasmas to maximize the clarity of the process.

We shall call the process coherent curvature radiation because the term is better known and more general. Our experiments use a hollow relativistic electron beam rotating with a speed $v = 0.95c$ and a radius of curvature $\rho = 3$ cm ($\sim$the Larmor radius), so we are in fact observing coherent synchrotron radiation. Streaming between beam and a nonrelativistic background plasma produces a strong instability at the upper hybrid frequency, which is slightly above the plasma frequency. The resulting bunching, driven by the electrostatic instability, forms a spatial array, as in radio antennas. The bunches can cooperate with each other, in the sense of having the same phase relation in their emission, if they lie within the same radiating cone, which has opening angle γ^{-1}, with γ the relativistic energy factor. The bunches lie along the helix followed by the gyrating beam (pitch angles typically exceeding 60°, and ranging up to 85°). However, because this cone includes only two or three bunches at best (defining a bunch as being one emitted wavelength long, typically 0.8 cm), this cooperative effect is of no importance in our laboratory work. However, it may be important in pulsars, where the number of cooperating bunches can be in the thousands.

This paper presents our investigations of this mechanism to date. We have eliminated to our satisfaction competing explantions of the emission. Observed power reaches several MW. Further studies in the future may enable us to turn this procedure around, so that the radiation can serve as a probe of the nonlinear turbulent spectrum of beam-plasma instabilities, enabling plasma physicists to study these complex problems in a nonperturbing way.

II. THEORY OF COHERENT CURVATURE RADIATION

The detailed theoretical model that initiated this work was given by Buschauer and Benford. [4] Here, we shall review briefly some basic points.

Relativistic electrons moving in a helical trajectory radiate cyclotron harmonic radiation. [1,2] The radiated power is [3]

$$P_1 = \frac{2}{3}\frac{e^2 c}{\rho^2}\beta_\theta^4 \gamma^4, \tag{1}$$

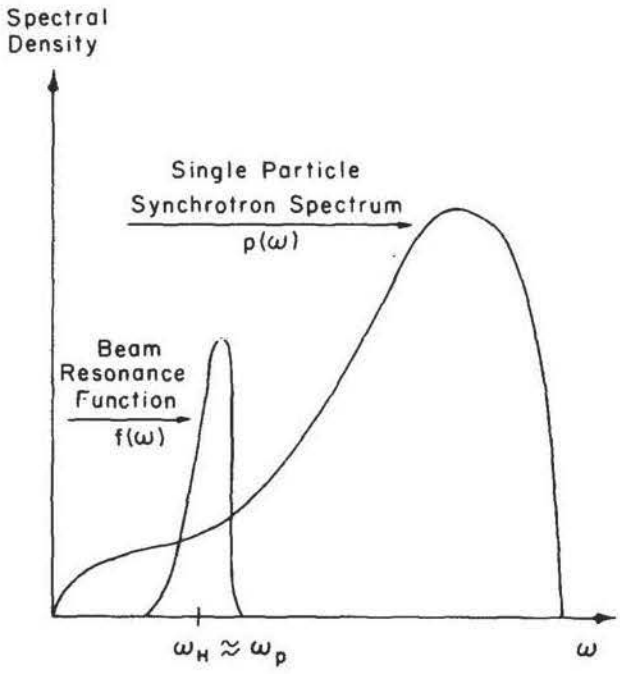

FIG. 1. The power and the two-stream instability spectra.

 0021-8979/79/106241-06$01.10

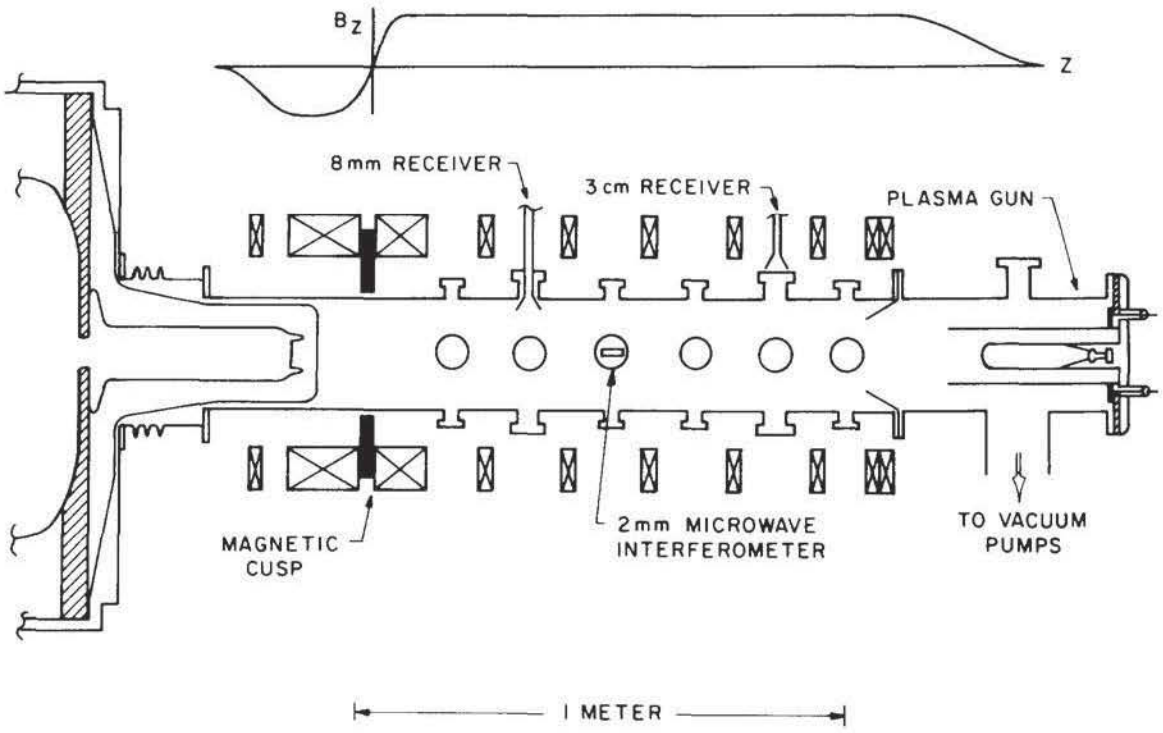

FIG. 2. Experimental appratus.

where $\beta_\theta c$ is the azimuthal velocity, $\gamma = (1-\beta^2)^{-1/2}$, and the radius of curvature, ρ, is

$$\rho = \frac{\gamma v_\theta}{\omega_c}\left(1+\frac{v_z^2}{v_\theta^2}\right)^{1/2}, \tag{2}$$

ω_c being the cyclotron frequency, eB/mc. The radiation spectrum $P(\omega)$ is shown in Fig. 1. The power peaks at a frequency

$$\omega^*/2\pi \cong \gamma^3 c/\rho. \tag{3}$$

The radiation is nearly tangential to the trajectory and is partially polarized. When an electron beam spirals in a plasma, a two-stream instability develops and causes the beam electrons to bunch. The bunched electrons then radiate their cyclotron radiation coherently, increasing the radiated power by a factor of ϵ given by [4]

$$\epsilon = \eta \rho A_t \tilde{n}/(2\gamma^3), \tag{4}$$

where A_t is the area of the beam bunches, transverse to the beam electron velocity, and $\tilde{n}$ is the fluctuation in the density of the beam due to the streaming instability. The total power for N electrons [using Eqs. (1) and (4) and approximating $\rho \cong \gamma v_\theta/\omega_c$] is

$$P_t = N\epsilon P_1 = \tfrac{1}{3} N\pi A_t \tilde{n} e^2 \omega_c \beta_\theta^3, \tag{5}$$

the power depends strongly on the magnetic field B since

$$\beta_\theta = \frac{v_\theta}{c} = \frac{eB}{mc^2}\frac{r_0}{\gamma}. \tag{6}$$

Here r_0 is the radius of the annulus of the electron beam. The two-stream instability occurs at the upper hybrid frequency $\omega_H^2 = \omega_p^2 + \omega_c^2$ (in our experiments $\omega_p^2 \gg \omega_c^2$ and $\omega_H \cong \omega_p$).

The estimated spectral function $f(\omega)$ of the two-stream instability is shown in Fig. 1. This function is much narrower than $P(\omega)$. [The width of $f(\omega)$ is probably given in our experiments by the variation in ω_H over a wavelength λ of the radiation, i.e., $\delta\omega \approx (\partial\omega_H/\partial_r)\lambda \approx (\partial\omega_p/\partial_r)\lambda \approx (\pi c/n)(\partial n/\partial r)$.] This is typically $\sim 0.1\omega_p$ for our experiments, so the overlap of $P(\omega)$ and $f(\omega)$ should give a fairly sharp profile of $P(\omega)$. By changing ω_H we can sweep $P(\omega)$ with $f(\omega)$. When $\omega_H \gg \omega^*$, the two spectra do not overlap and no coherent radiation is expected. However, as ω_H decreases $f(\omega)$ starts to overlap $P(\omega)$ and a rapid increase in radiated power is expected. The radiation will peak when $\omega_H = \omega^*$ and will decrease slowly as ω_H decreases below ω^*.

III. THE EXPERIMENTAL SYSTEM

The experimental apparatus and the magnetic field shape are shown in Fig. 2.

From the right end of the drift tube a plasma gun is fired, filling the tube with plasma. (Part of the experiments were carried out with a Marshall gun [5] and the remainder where with a titanium stacked washer gun. [6]) A 2-mm microwave interferometer monitors the density continuously. At a later time, we fire an annular electron beam (typically $V = 1$ MV, $I = 30$ kA, radius $r_0 = 3$ cm, and thickness $t = 0.5$ cm) through an anode foil and a magnetic cusp. The beam then spirals through the plasma and interacts with it. A *Ka* band horn couples the microwave radiation into a 10m waveguide, leading to the screen room, where the signal is attenuated and detected. A 35-m dispersive delay line is used to measure the radiated frequency. The waveguide has a cutoff frequency of 21 GHz and single-mode operation up to

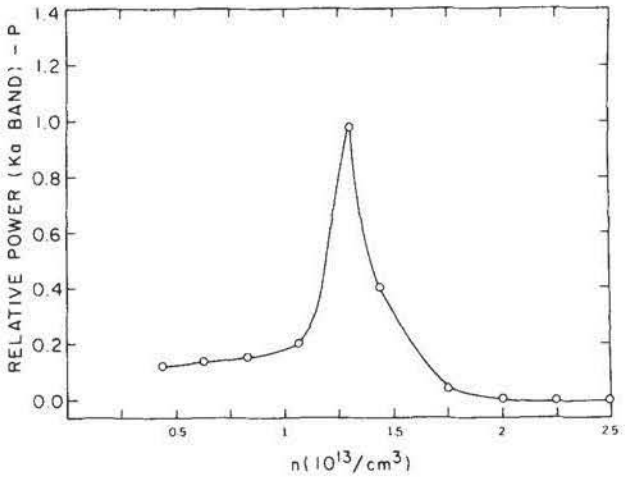

FIG. 3. Radiated power versus n_p.

42 GHz. Radiation was also monitored in frequency bands 8–26.5 and 110–170 GHz.

An x-ray pin diode array was used to confirm beam propagation and monitor the beam profile. In part of the experiments we inserted a Lucite damage rod into the beam path to confirm beam rotation and measure the pitch angle. [7]

IV. EXPERIMENTS

In the experiments described below, we used two types of plasma sources, a Marshall gun and a titanium stacked washer gun. We used two electron beam machines, one with a 110-nsec pulse width and the other with a 1-μsec pulse width. The Marshall gun produces many neutral atoms in addition to the plasma. When the beam passes through, it ionizes these neturals and the plasma density changes significantly. This sudden change implies that the matching condition, $\omega_H = \omega^*$, exists for only a short time and the microwave pulses are short. The use of the titanium stacked washer gun, which does not emit many neutrals, enables us to overcome this problem, and we got microwave radiation during the full length of the electron beam pulse for both the short and the long electron beam pulse.

A. Output power versus plasma density

In the first series of experiments we fired a Marshall plasma gun into the drift tube and after a certain elapsed time we fired an annular rotating electron beam. By varying the time delay t_d between the gun and the beam, we controlled the plasma density, and hence, the plasma frequency. The magnetic field was set to 1.5 kG, and the pitch angle was $\sim 65°$. A 2-mm interferometer was used to monitor the plasma frequency continuously. We searched for radiation in the frequency range between 8 and 170 GHz. A significant amount of power was detected in the *Ka* band only. In all other band, the power was down by two orders of magnitude at least.

The radiated power versus density is plotted in Fig. 3. At low plasma frequencies, the power rises slowly as ω_p is increased. When $\omega_p/2\pi$ approaches 30 GHz we get a sharp increase in power and when ω_p is further increased the power drops rapidly and decreases by two orders of magnitude as $\omega_p/2\pi \sim 50$ GHz. This behavior is in good agreement with the theoretical graphs described in Fig. 1. When we sweep $P(\omega)$ with $f(\omega)$ we expect the power to increase slowly as ω_p increases (towards ω^*), a peak at $\omega_p = \omega^*$, and a sharp decrease for $\omega_p > \omega^*$.

A typical negative polarity signal is shown in Fig. 4. Pulse No. 1 is the *Ka* band detected pulse entering the delay line. Pulse No. 2 is the detected signal at the delay line output. Since the line is dispersive, one can determine the frequency by measuring the time delay.

The frequency gap between successive spikes is 1.7 GHz, which is in good agreement with the harmonic structure expected from relativistic electrons moving in a helical trajectory. This spacing is given by

$$\frac{\Delta\omega}{2\pi} = \frac{\omega_c}{2\pi\gamma \sin^2\theta},$$

where θ is the pitch angle. Here $\theta = 65°$, $B = 1.5$ kG, and thus

$$\Delta\omega/2\pi \cong 1.5 \text{ GHz}.$$

The nonrelativistic harmonic spacing is

$$\omega_c/2\pi \cong 4.2 \text{ GHz}.$$

The observed harmonic spacing implies that we are dealing with direct radiation from the beam electrons and not conversion of electrostatic waves in the boundary, [8,9] which would have the nonrelativistic harmonic spacing.

We estimated the total power by multiplying the power coupled into the horn by the ratio of drift-tube area to horn area. The power coupled into the horn by the three most powerful harmonics in Fig. 4 is 400, 160, and 140 W, respectively. The area ratio was ~ 2000; thus, the total power exceeds 1 MW.

An important result of this experiment is the fact that when $\omega_p > \omega^*$ there was *no* radiation in neither the *Ka* band nor the higher-frequency bands, indicating that the resonance condition $\omega_H \cong \omega^*$ is essential.

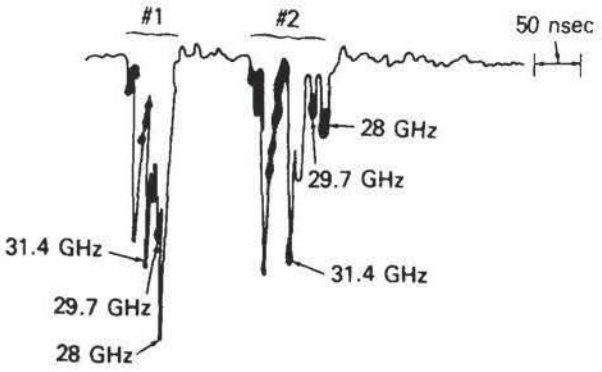

FIG. 4. Oscillogram of the sum of undelayed *Ka* band detected pulse (No. 1) and the delayed and dispersed pulse (No. 2).

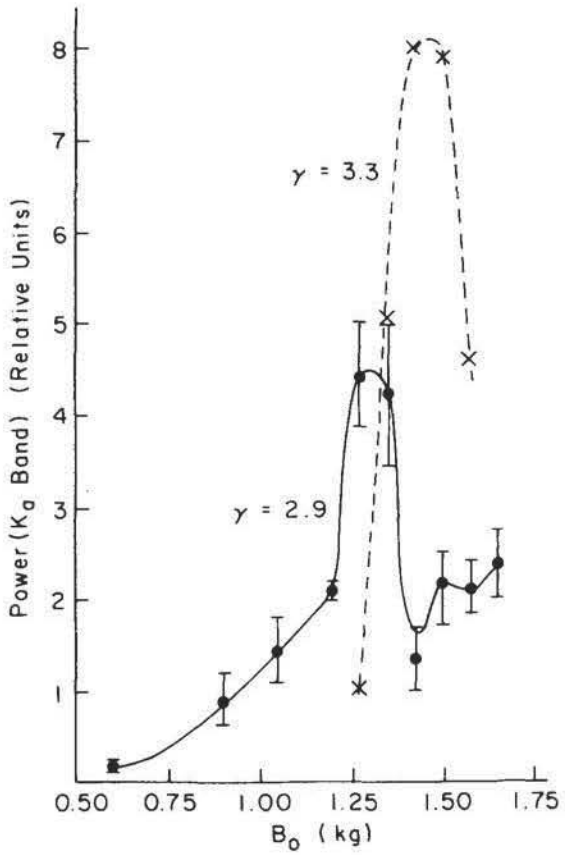

FIG. 5. Radiated power versus magnetic field for $\gamma = 2.9$ and $\gamma = 3.3$.

B. Output power versus magnetic field

In a second series of experiments, ω_p was kept approximately constant at its optimal value in Fig. 3, while the magnetic field B was varied. This implies variation of the ratio v_θ/v_z, which affects the output power strongly [Eqs. (5) and (6)]. Unfortunately, there is a limit on B due to the cusp cutoff field B_{cr} at which, ideally, all of the initial velocity is converted into rotational velocity, and the beam stops propagating. B_{cr} is given by

$$B_{cr} = \frac{mc\gamma}{er}(1-\gamma^{-2})^{1/2}. \tag{7}$$

In this experiment we keep the curve $f(\omega)$ in Fig. 1 constant, while the increasing B we increase ω^* in Eq. (3). Thus, for a low magnetic field the curve $P(\omega)$ (Fig. 1) does not overlap $f(\omega)$ and no coherent radiation is expected. As we increase B, the curve $P(\omega)$ becomes wider and starts to overlap $f(\omega)$. We thus expect a steep onset of radiation. When we further increase B, we approach B_{cr} and radiated power starts dropping due to beam cutoff. The experimental curves in Fig. 5 show good agreement with this prediction, for both $\gamma = 3.3$ and $\gamma = 2.9$, although the onset of radiation for $\gamma = 2.9$ is not as fast as the fourth power dependence shown in Eq. (5). The peak in power occurs at a higher B for $\gamma = 3.3$ than for $\gamma = 2.9$ since B_{cr} increases with γ.

For $B = 1.28$ kG, the power for $\gamma = 3.3$ is less than that for $\gamma = 2.9$ by a factor of ~ 0.62, in agreement with Eqs. (5) and (6) since $P_t \sim \beta_\theta^3$, $\beta_\theta \sim (\gamma)^{-1}$, and $(2.9/3.3)^3 \cong 0.67$.

On the other hand, the peak power for $\gamma = 3.3$ is greater than that for $\gamma = 2.9$ by a factor of ~ 1.7, while the corresponding magnetic fields are 1.28 and 1.47 kG. The current density and hence N (the number of radiating particles) increased by 1.7 and the product $N\omega_c\beta_\theta^3$ [in Eq. (5)] increased by ~ 1.5. Thus the calculated power should increase by ~ 1.5 (assuming no change in $\tilde{n}A_t$), which is fairly close to the measured ratio of 1.7. (This suggests $\tilde{n}A_t$ is insensitive to γ.) It should be mentioned here that *no Ka* band radiation was observed when we fired the beam into a constant magnetic field (with no cusp). In this case there is little rotation of the electrons, and hence little curvature radiation is expected. This dramatic reduction in radiated power when the cusp is deactivated indicates that beam rotation is essential. This would not be the case, for example, if we were observing $\omega \approx \omega_p$ radiation from scattering off ions, as is seen in type-III solar bursts.

C. Extension of microwave pulse length to that of the beam

As can be seen in Fig. 4, in some cases the microwave pulse consisted of several short spikes. In other cases we had a single short pulse, as in Fig. 6(b). This pulse is much shorter than the beam pulse shown in Fig. 6(a). We suspected this was because the matching condition $\omega_p \cong \omega^*$ lasted for only a short time, because of a sudden change in ω_p when the beam passes through the plasma. We can see this change on the interferometer trace in Fig. 6(c). At the beginning, the plasma density is higher than the cutoff density for the 2-mm wave and no fringes can be seen. Then fringes appear, and later the density decreases and the fringes become more widely spaced. When the beam is fired, the density jumps into the cutoff region again, and later starts to decrease once again. We believe that the reason for this change in density is

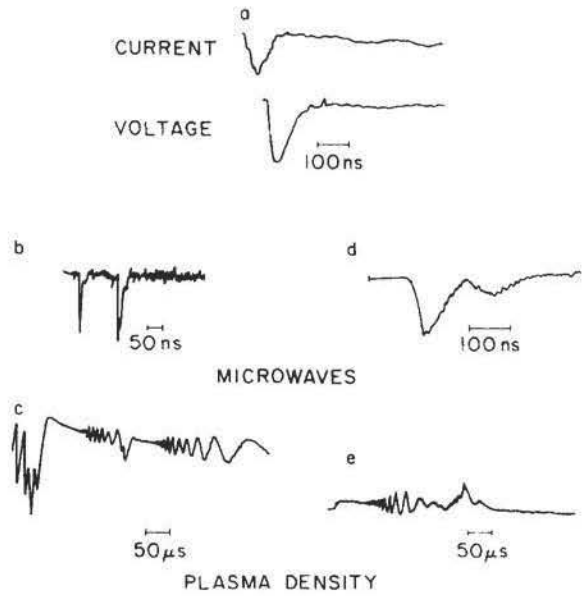

FIG. 6. Short pulse machine experiments: (a) Current and voltage traces, (b) microwave pulse with Marshall gun, (c) interferometer trace with Marshall gun, (d) microwave pulse with washer stack gun, and (e) interferometer trace with washer stack gun.

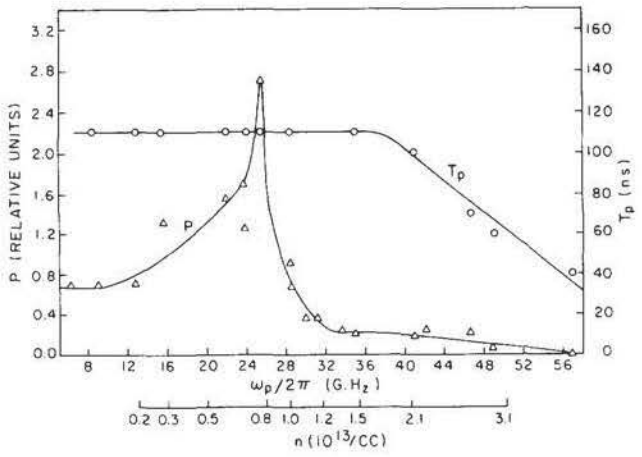

FIG. 7. Pulse length and output power versus density.

the ionization by the beam of the many neutrals emitted by the Marshall gun.

To prevent this sudden change in density when the beam is fired, we used a titanium washer stack gun which does not emit many neturals. The interferometer trace for this gun is shown in Fig. 6(e). When the beam is fired, we see only an electrostatic noise spike and then the density trace continues without any change. The microwave pulse in this case [Fig. 6(d)] is as long as and is similar to the beam-voltage trace [Fig. 6(a)].

In Fig. 7 we plotted the dependence of the microwave pulse length on the plasma density, n (or plasma frequency $\omega_p/2\pi$), for the stack washer gun. As can be seen there the pulse length is equal to that of the beam voltage for densities below $1.5\times10^{13}/\text{cm}^3$. For higher densities, the density started to change when the beam was fired and the microwave pulse width started to decline. In Fig. 7 we also show the radiated power versus density (in another series of experiments). The power peaks well below $1.5\times10^{13}/\text{cm}^3$ so that at the peak power we also get the full pulse length. Thus the energy peaks when the power does.

D. 1-μsec-long pulses

We conducted a similar series of experiments on our long-pulse machine [10] in which we have a 1-μsec pulse of 0.6 MV and 15-kA peak current. The results were quite similar to those of the short-pulse experiments for both the Marshall gun and the washer stack gun. Figure 8(a) shows the voltage trace and Fig. 8(c) shows the interferometer trace for a Marshall-gun shot. Here again we see the great change in density when the beam is fired. The microwave pulse in this case [Fig. 8(b)] consists of several short spikes which last altogether much less than the beam. In Fig. 8(e) we see a density trace of a shot taken with the washer stack gun. The density here does not change when the beam is fired (except from the noise pickup) and the microwave pulse lasts for about 1 μsec and is similar to the voltage pulse. It should be noted here that the voltage pulse is spiky here and so is the microwave pulse. This probably represents "jitter" around the resonance condition $\omega^* = \omega_p$ caused by fluctuations in the voltage (and in γ).

V. DISCUSSION

The incoherent radiated power from N electrons, calculated by multiplying Eq. (1) by N, yields in our case ~ 1 W. Since the power levels in these experiments exceeded 1 MW, we are obviously dealing with a coherent process.

Assuming in Eq. (5),[4] $A_t = 0.1\ \text{cm}^2$, $\tilde{n}/n = 0.01$, and $n_b = 1.7\times10^{11}$ we get $P_t \cong 50$ MW. This means that we are well below a resonable maximum attainable power. In addition, we expect to be able to increase the radiated frequency by increasing γ and decreasing ρ in Eq. (3).

The harmonic structure of the radiation exludes the possibility of radiation from electrostatic waves converted into electromagnetic waves at the plasma boundary,[8,9] as was explained in Sec. IV A. The harmonic structure is also different from those in both the Astron experiments [12] and the rotating electron beam in vacuum[13,14] where the radiation peaked at $l\sim\gamma$, where l is the harmonic of the beam cyclotron frequency. Here we observed a much higher harmonic number, namely, $l\sim\gamma^3$.

We can understand the pronounced peak in Fig. 7 by noting that when $\omega_p > \omega^*$, the power should decline exponentially because the single-particle emission function does.[4] The low level of power at higher densities probably results from emission in regions at large radii with lower plasma density. These regions will give coherent radiation because $\omega_p < \omega^*$ there, even though $\omega_p > \omega^*$ at the center of the drift tube. The peak should occur where $\omega^*/2\pi = 21.5$ GHz $= \omega_p/2\pi$. The observed peak at ~ 25 GHz (Fig. 7) probably corresponds to experimental variance in γ and plasma densi-

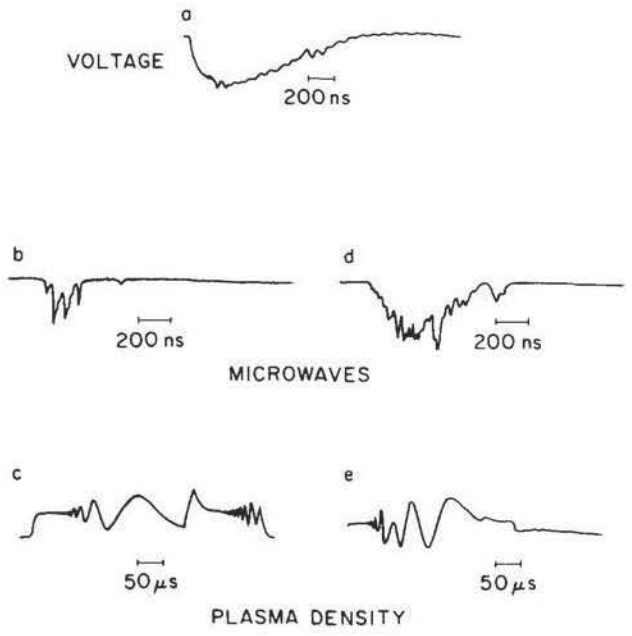

FIG. 8. Long-pulse machine experiments: (a) voltage, (b) microwave pulse with Marshall gun, (c) interferometer with Marshall gun, (d) microwave pulse with washer stack gun, and (e) interferometer trace with washer stack gun.

ty. The slope of the left side of the peak agrees qualitatively with the Buschauer and Benford [4] calculations, Eq. (33). The power scales as N^2/S_0 where $N = n_b V$, V is the volume of the emitting clumps, n_b is the beam density, and S_0 is the coherence length along θ for the rotating beam. Now, $V = \xi\eta S_0$ where ξ and η are the transverse dimensions of the clumps; they should be set by the velocity spread of the beam (which dephases waves if they are moving at the differing beam-particle velocities) and by dephasing effects due to inhomogeneities in n_p. The variation $\delta n_p/n_p$ should decline with n_p, so we would expect $\xi\eta$ to increase with n_p. A slow scaling $(\xi\eta) \sim n_p$ can easily account for the rise in power seen on the left face of the peak in Fig. 7.

VI. CONCLUSION

We observed high-power microwave pulses with properties in good agreement with the theory of coherent curvature radiation. The pulse length, very short in the earlier stages of this reasearch, was shown to result from the experimental setup, rather than from an inherent property of the mechanism responsible for the radiation. By a proper choice of the plasma source we extended the microwave burst length to that of the electron beam, for beam pules as long as 1 μsec. This suggests the possibility of getting even longer microwave pulses with longer beam pulses. We also anticipate getting higher power levels by increasing the magnetic field, generating rotation in the beam by firing the beam into an increasing magnetic field (avoiding thus the cusp cutoff problem). The process also recommends itself for production of higher frequencies by increasing γ and decreasing ρ.

ACKNOWLEDGMENTS

The authors are grateful to A. Fisher for helpful discussions and to D. Affinito for his help in assemblying the experiment. We appreciate the great help of V. Granatstein in the initial stages of this work. Very fruitful discussions with J. Schneider are appreciated.

[1] G. Bekefi, *Radiation Processes in Plasmas* (Wiley, New York, 1966), p. 177.
[2] J.D. Jackson, *Classical Electrodynamics* (Wiley, New York, 1975), p. 654.
[3] J.D. Jackson, Ref. 2, p. 661.
[4] R. Buschauer and G. Benford, Mon. Not. R. Astron. Soc. **177**, 109 (1976).
[5] J. Marshall, Phys. Fluids **3**, 134 (1960).
[6] R.S. Lowder and F.C. Hoh, Rev. Sci. Instrum. **33**, 1236 (1962).
[7] C.W. Roberson, G. Saenz, and D. Tzach, Rev. Sci. Instrum. **48**, 31 (1977).
[8] C.D. Stifler and T. Kammash, Plasma Phys. **15**, 729 (1973).
[9] S. Gruber and G. Bekefi, Phys. Fluids **11**, 123 (1968); B.R. Kusse and A. Bers, Phys. Fluids **13**, 2372 (1970).
[10] F. Levin and A. Fisher, Bull. Am. Phys. Soc. **21**, 1097 (1976).
[11] V. Granatstein, C. Roberson, G. Benford, D. Tzach, and S. Robertson, Appl. Phys. Lett. **32**, 88 (1978).
[12] T.J. Fessenden and B.W. Stallard, Lawrence Radiation Laboratory, Controlled Thermonuclear Research Annual Report UCRL-50002-70, 1970, p. 3–27.
[13] V.L. Granatstein, R.K. Parker, and P. Sprangle, Sandia Laboratories Document SAND 76-5122, 1975, Vol. II, p. 401.
[14] P. Sprangle, J. Appl. Phys. **47**, 2935 (1976).